European Journal of Neuroscience, Vol. 24, pp. 419–432, 2006 doi:10.1111/j.1460-9568.2006.04914.x

Inhibition of constitutive inward rectifier currents in cerebellar granule cells by pharmacological and synaptic activation of $GABA_B$ receptors

Paola Rossi,[1] Lisa Mapelli,[1] Leda Roggeri,[1] David Gall,[1,2] Alban de Kerchove d'Exaerde,[2] Serge N. Schiffmann,[2] Vanni Taglietti[1] and Egidio D'Angelo[1]
[1]Department of Cellular-Molecular Physiological and Pharmacological Sciences, University of Pavia, Via Forlanini 6, I-27100, Pavia, Italy
[2]Laboratoire de Neurophysiologie (CP601), Facultè de Mèdecine, Universitè Libre de Bruxelles, Route de Lennik 808, B-1070 Bruxelles, Belgium

Keywords: cerebellum, $GABA_B$ receptors, granule cells, inward rectifier, non-synaptic plasticity

Abstract

γ-Aminobutyric acid $(GABA)_B$ receptors are known to enhance activation of Kir3 channels generating G-protein-dependent inward rectifier K^+-currents (GIRK). In some neurons, $GABA_B$ receptors either cause a tonic GIRK activation or generate a late K^+-dependent inhibitory postsynaptic current component. However, other neurons express Kir2 channels, which generate a constitutive inward rectifier K^+-current (CIRK) without requiring G-protein activation. The functional coupling of CIRK with $GABA_B$ receptors remained unexplored so far. About 50% of rat cerebellar granule cells in the internal granular layer of P19–26 rats showed a sizeable CIRK current. Here, we have investigated CIRK current regulation by $GABA_B$ receptors in cerebellar granule cells, which undergo GABAergic inhibition through Golgi cells. By using patch-clamp recording techniques and single-cell reverse transcriptase-polymerase chain reaction in acute cerebellar slices, we show that granule cells co-express Kir2 channels and $GABA_B$ receptors. CIRK current biophysical properties were compatible with Kir2 but not Kir3 channels, and could be inhibited by the $GABA_B$ receptor agonist baclofen. The action of baclofen was prevented by the $GABA_B$ receptor blocker CGP35348, involved a pertussis toxin-insensitive G-protein-mediated pathway, and required protein phosphatases inhibited by okadaic acid. $GABA_B$ receptor-dependent CIRK current inhibition could also be induced by repetitive GABAergic transmission at frequencies higher than the basal autorhythmic discharge of Golgi cells. These results suggest therefore that $GABA_B$ receptors can exert an inhibitory control over CIRK currents mediated by Kir2 channels. CIRK inhibition was associated with an increased input resistance around rest and caused a $\sim$5 mV membrane depolarization. The pro-excitatory action of these effects at an inhibitory synapse may have an homeostatic role re-establishing granule cell readiness under conditions of strong inhibition.

Introduction

The inward rectifiers include different classes of K^+-permeable channels widely expressed in neurons and other excitable cells. By activating with hyperpolarization, inward rectifiers can be involved in various cell functions, from stabilizing resting membrane potential to regulating subthreshold excitatory postsynaptic potential integration and repetitive spike discharge. There are two main classes of K^+-permeable inward rectifier channels, Kir2 and Kir3. Kir3 channels, due to their G-protein dependence, are often called G-protein-dependent inward rectifier K^+-currents (GIRK). GIRK can be activated by several neurotransmitters including γ-aminobutyric acid (GABA), which, by activating $GABA_B$ receptors (Dutar & Nicoll, 1988; Misgeld *et al*., 1995; Nicoll, 2004), can generate either a tonically active inward rectifier K^+-current (Chen *et al*., 2004; Chen & Johnston, 2005) or a delayed K^+-dependent component of the inhibitory postsynaptic currents (IPSCs) (Dutar & Nicoll, 1988; Connors *et al*., 1988). Inward rectifier channels of the Kir2 family are also highly expressed in the brain (Chandy & Gutman, 1993; Stanfield *et al*., 2002; Pruss *et al*., 2005). Kir2 are stronger rectifiers than Kir3 channels and are constitutively active (CIRK). Although CIRK channels can be regulated by muscarine and substance P (Velimirovic *et al*., 1995; Wang & McKinnon, 1996), and are sensitive to the phosphorylative balance (Inoue & Imanaga, 1995; Takano *et al*., 1995; Kamouchi *et al*., 1997), their regulation by $GABA_B$ receptors has not been reported so far.

In cerebellar granule cells, GIRK currents activated by $GABA_B$ receptors and GTPγS are observed at a premigratory stage. GIRK currents play a key role for granule cell maturation and survival, and their mutation (in Kir3.2 or GIRK-2) causes the *weaver* degeneration (Kofuji *et al*., 1996; Rossi *et al*., 1998). Although *in situ* hybridization and immunostaining reveals Kir3 channels also in the mature cerebellum (e.g. Karschin *et al*., 1996; Liao *et al*., 1996), the phenotype of inward rectifier currents switches from GIRK to CIRK as granule cells migrate from the external to internal granular layer (D'Angelo *et al*., 1995; Armano *et al*., 2000; Mathie *et al*., 2003). The CIRK current is Ba^{2+}-sensitive with steep voltage dependence, and Kir2.2 channel mRNA and protein have indeed been revealed by *in situ* hybridization (Karschin *et al*., 1996; Horio *et al*., 1996) and

Correspondence: Dr E. D'Angelo and Dr P. Rossi, [1]Department of Cellular-Molecular Physiological and Pharmacological Sciences.
E-mail: dangelo@unipv.it and prossi@unipv.it

Received 24 December 2005, revised 25 March 2006, accepted 5 May 2006

immunohistochemistry (Stonehouse *et al.*, 1999). Biochemical assays have shown that Kir2 channels in granule cells are coupled to complex transduction molecular complexes (Leonoudakis *et al.*, 2001, 2004). $GABA_B$ receptors have also been revealed in mature granule cells by *in situ* hybridization and immunohistochemistry (Ige *et al.*, 2000; Liang *et al.*, 2000). $GABA_B$ receptors may be physiologically activated by Golgi cells, which are GABAergic interneurons know to activate $GABA_A$ receptor-mediated responses in granule cells (Edgley & Lidierth, 1987; Brickley *et al.*, 1996; Dieudonne, 1998; Vos *et al.*, 1999a,b; Rossi *et al.*, 2003; Dugue *et al.*, 2005). Thus, the mature granule cell circuit appears to combine Kir3 channels with $GABA_B$ receptors, although their functional coupling remained to be investigated.

In this paper, the co-localization of $GABA_B$ receptors and Kir2 channels was demonstrated by single-cell reverse transcriptase-polymerase chain reaction (RT-PCR). Surprisingly enough, both pharmacological and synaptic activation of $GABA_B$ receptors inhibited the CIRK current, depolarizing the membrane at rest and increasing subthreshold input resistance. These effects, which are apparently in contrast with the well-known inhibitory effect of GABAergic synapses, may play an important role for regulating the inhibitory action of Golgi cells on granule cells.

Materials and methods

Slice preparation and recording procedures

Patch-clamp recordings were performed from granule cells in the granular layer of cerebellar slices using either the whole-cell or perforated-patch technique (Horn & Marty, 1988). Cerebellar slices (250 μm thick) were obtained from postnatal day (P)19–26 rats (Wistar strain, day of birth = 1) as reported previously (D'Angelo *et al.*, 1995, 2001; Rossi *et al.*, 1998; Armano *et al.*, 2000). Briefly, the animals were anaesthetized with halothane and killed by decapitation (the experimental procedure was approved by the Ethical Committee of the University of Pavia). Slices were cut and maintained in Krebs solution (in mM): NaCl, 120; KCl, 2; $MgSO_4$, 1.2; $NaHCO_3$, 26; KH_2PO_4, 1.2; $CaCl_2$, 2; glucose, 11; and was equilibrated with 95% O_2 and 5% CO_2 (pH 7.4). In some experiments slices were maintained overnight in Krebs solution (pH 7.4 by bubbling with 95% O_2 and 5% CO_2, room temperature) added with pertussis toxin (PTX, 5 μg/mL, Chen *et al.*, 2001). During recordings the slices were superfused with oxygenated Krebs and maintained at 30 °C with a Peltier feedback device (HCC-100A; Dagan, Minneapolis, MN, USA). Test solutions were applied locally through a multibarrel pipette, in which Krebs was added with ionotropic and metabotropic glutamate receptor antagonists [in μM: 6-cyano-7-nitroquinoxaline-2,3-dione (CNQX), 10; D-2-amino-5-phosphonovaleric acid (APV), 100; 7-chlorokinurenic acid (7-Cl-kyn), 50; (+)-α-methyl-4-carboxyphenyl-glycine (MCPG), 500] and, in some cases, with ionotropic and metabotropic GABA receptor antagonists (in μM: bicuculline, 30; CGP35348, 50; Barthel *et al.*, 1996). Nystatin, bicuculline and GTPγS were obtained from Sigma (St. Louis, MO, USA). R-baclofen (Barthel *et al.*, 1996), CGP35348, APV, 7-Cl-kyn, CNQX and MCPG were obtained from Tocris Cookson (Bristol, UK). Okadaic acid (Inoue & Imanaga, 1995; Kamouchi *et al.*, 1997; Alexis, San Diego, CA, USA) was dissolved in dimethylsulphoxide. PTX was delivered from List Biological Laboratorie (California, USA).

For whole-cell recording (WCR), pipettes were filled with the following intracellular solution (in mM): K-gluconate, 126; NaCl, 4; $MgSO_4$, 1; $CaCl_2$, 0.02; BAPTA, 0.1; glucose, 15; ATP, 3; HEPES, 5 (pH was adjusted to 7.2 with KOH), and either 0.1 mM GTP or GTPγS. Considering that this solution was diluted by 10% before use (Rossi *et al.*, 1998), and assuming a 0.75 activity coefficient for K^+ salts, the nernstian reversal potential for K^+ ions was −85.7 mV (Pitzer & Mayorga, 1973). Intracellular Ca^{2+} was buffered at 100 nM. In some recordings the perforated-patch technique was used to prevent cytoplasmic washout and maintain the endogenous Ca^{2+} buffer (Horn & Marty, 1988). The pipette solution used for perforated-patch recording (PPR) contained nystatin 100 μg/mL and (in mM): K^+-sulphate, 84; NaCl, 4; glucose, 30; HEPES, 5 (pH was adjusted to 7.2 with KOH). The membrane potential was corrected for the Donnan potential developing across the patch (−9.8 mV inside the cell).

Golgi cell axon stimulation was performed using a patch-pipette positioned in the internal granular layer through a stimulus isolation unit. Signals were recorded with an Axopatch-200B amplifier, sampled with a Digidata-1200 interface and analysed with pClamp software (Axon Instruments, Foster City, CA, USA). Data are reported as mean ± MSE, and statistical comparisons were made using Student's *t*-test. Differences were considered significant at $P < 0.05$.

Voltage-clamp recordings

To measure CIRK currents, hyperpolarizing voltage steps were given from the holding potential of −40 mV, and voltage-ramps were raised at 0.08 mV/ms from the holding potential of −120 mV. The presence of CIRK currents was revealed by inward rectification in the negative membrane potential region. In practice, a cell was considered as expressing CIRK currents when the $\Delta I/\Delta V$ ratio in the −120 mV to −100 mV range was 10% greater than in the −54 mV to −60 mV range. In order to minimize run-down problems, all pharmacological and stimulation protocols have been started between 3 and 6 min from the establishment of the whole-cell recording configuration, when CIRK current amplitude tends to stabilize. Time is set at 0 at the beginning of the protocols and CIRK current amplitude is measured relative to the last control point.

Passive properties

Current transients elicited by −10 mV voltage steps from the holding potential of −70 mV showed a fast mono-exponential relaxation indicating that granule cells behaved as single electrical compartments. The transients were used to estimate series resistance (18.6 ± 2 MΩ, $n = 21$), input resistance (2.9 ± 0.5 GΩ, $n = 21$) and membrane capacitance (4.4 ± 1.2 pF, $n = 21$), yielding typical values of granule cells (D'Angelo *et al.*, 1995).

Leakage subtraction and CIRK conductance curve

Currents activated by depolarizing ramps were used to obtain current–voltage (*I–V*) plots, which were fitted with the following equation:

$$I(V) = [G_{IR}(V_m - E_K)]/[1 + \exp((V_m - V_{1/2})/k)] + [G_L(V_m - E_L)], \quad (1)$$

where G_{IR} is the maximum CIRK conductance, V_m is the membrane potential, E_K is the Nernst potential for K^+, $V_{1/2}$ is the potential at which CIRK conductance is half-activated and k is the voltage dependence of its activation, G_L is the linear leakage conductance and E_L is the leakage reversal potential (Hille & Schwarz, 1978). For curve fitting, E_K was fixed to −85.7 mV while the other parameters were left free. When also E_K was left free to vary, it assumed values within ± 10 mV of its theoretical value, supporting the K^+ dependence of the current. Curve fitting with Eqn 1 (e.g. Fig. 1B) was performed between −120 mV and −60 mV by least-squares minimization

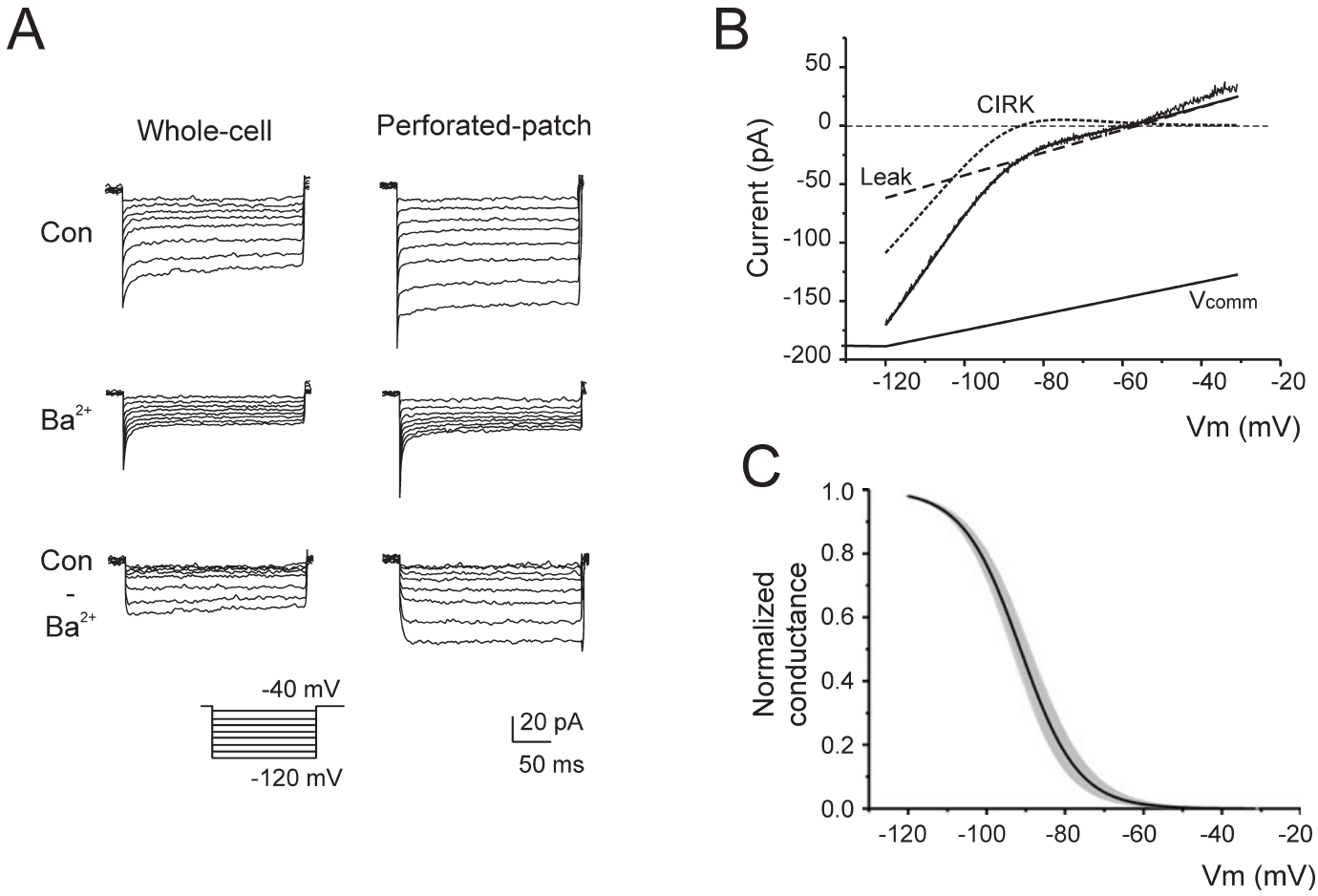

FIG. 1. Constitutive inward rectifier current (CIRK) in mature cerebellar granule cells. (A) CIRK currents elicited by step-hyperpolarization from the holding potential of −40 mV in whole-cell and perforated-patch recordings. The current was blocked by 1 mM Ba^{2+}. The Ba^{2+}-sensitive currents were obtained by digital subtraction (con-Ba^{2+}). (B) CIRK currents elicited by voltage-ramp (V_{comm}) before (continuous line) and after (broken line) subtraction of the leakage current [see Eqn 1]. A fitting function is superimposed to the experimental tracing. CIRK parameters: $V_{1/2} = -91$ mV, $k = 9/$mV, $G_{IR} = 3.3$ nS, $E_K = -85.7$ mV (fixed). Leakage parameters: $G_L = 0.97$ nS and $E_L = -56.2$ mV. (C) Averaged normalized conductance curve ($n = 35$) constructed by Eqn 2. The shaded area indicates the MSE of curve fitting obtained from individual experiments.

(Origin, Microcal Software, Northampton, MA, USA). The fitting procedure converged to the same result independent of initial parameters, and none of the free parameters showed unusual variability. The average parameter values obtained from curve fitting were used to construct average activation curves (e.g. Fig. 1C) using the Boltzmann equation

$$G/G_{IR} = 1/[1 + \exp((V_m - V_{1/2})/k)] \quad (2)$$

The linear leak current obtained by Eqn 1 was subtracted from the experimental tracings in the rest of the paper following the procedure illustrated in Fig. 1B.

Current-clamp recordings

Current-clamp recordings were performed in the 'fast' operating mode of the Axopatch-200A to optimize the reaction rate of the amplifier (the procedure is described in D'Angelo *et al*., 1995). Membrane potential during step current injection was estimated as the average value between 500 and 800 ms.

Single-cell RT-PCR

In a specific set of experiments, cerebellar granule cells were visually identified with 63 × Nomarsky optics and patch-clamped 20–50 μm below the surface of the slice. After performing voltage-ramp protocols to identify the presence of CIRK currents, the cytoplasm was retrieved by aspiration into the recording pipette under visual control.

Cytoplasm harvest

The pipette solution contained (in mM): KCl, 144; $MgCl_2$, 3; EGTA, 0.2; HEPES, 10; 4, NaATP; NaGTP, 0.4 (pH adjusted at 7.2 with KOH). The contents were expelled into a test-tube where the RT reaction was performed in a final volume of 10 μL (Lambolez *et al*., 1992), left overnight at 37 °C. PCR amplification was performed for detection of the two $GABA_B$ receptor subunits 1 and 2 ($GABA_BR1$ and $GABA_BR2$), the alpha 6 subunit of the $GABA_A$ receptor ($GABA_A R\alpha 6$), and the three inwardly rectifying K^+ channels Kir 2.1, Kir2.2 and Kir 2.3. The possibility of contamination was ruled out by inclusion of a template minus negative control (extracellular solution near harvested neurons).

Multiplex RT-PCR

The set of primers used for $GABA_BR1$, $GABA_BR2$ and $GABA_A R\alpha 6$ were located in different exons to rule out genomic DNA amplification by size criterion. The sets of primers for Kir 2.1, 2.2 and 2.3 are

described in Mermelstein *et al*. (1998). The two steps of multiplex PCR were performed as described previously (Léna *et al*., 1999). The resulting cDNAs of $GABA_BR1$, $GABA_BR2$, $GABA_A R\alpha 6$, Kir 2.1, Kir 2.2 and Kir 2.3 contained in 10 μL RT reaction were first amplified simultaneously. *Taq* polymerase (2.5 U) (Qiagen, Germany) and 10 pmole of each of the 14 primers were added in the buffer supplied by the manufacturer (final volume 100 μL), and 20 cycles (94 °C, 1 min; 60 °C, 1 min; 72 °C, 1 min) of PCR were run. Second rounds of PCR were then performed using 2 μL of the first PCR as template (final volume 50 μL). In this second PCR, each cDNA was amplified individually using its specific primer pair by performing 40 PCR cycles as described above. Twenty microlitres of each individual PCR was then run on a 2% agarose gel. The efficiency of this multiplex RT-PCR protocol was tested on 10 pg of whole-brain total RNA (Léna *et al*., 1999; Porter *et al*., 1999).

The following sets of primers were used (from 5′ to 3′):

$GABA_BR1$
forward GGGTGGTATGCTGACAACTGGT,
reverse GCCCGGTAGATCTGGTCTGTAAT,
yielding a predicted PCR product of 355 bp;

$GABA_BR2$
forward GAAACCGCGAATGTGAGCAT,
reverse TCCCAAGTCTTTGTCCAGCTCTGT,
yielding a predicted PCR product of 401 bp.

Two sets of primers on different exons were used for $GABA_A R\alpha 6$:

$GABA_A R\alpha 6$
Forward1 CCGACAGACATGGACTGATGAG,
Reverse1 TTCGCTTTTCGGATAGGCATAG,
yielding a PCR product of 300 bp;

$GABA_A R\alpha 6$
Forward2 CAACGCTGACTGTCCGATGA,
Reverse2 GATGCACGGAGTGTAAATCTGGAT,
yielding a PCR product of 300 bp.

The sets of primers for inwardly rectifying K^+ channels are:

Kir2.1
Forward AAGCAGGACATTGACAATGCAGAC,
Reverse AGGTGAGTCTGTGCTTGTGCTCT,
yielding a PCR product of 359 bp;

Kir2.2
Forward ATCATCTTCTGGGTCATTGCTGTC,
Reverse CGTCTCGAGGTCCTGACGGCTAAT,
yielding a PCR product of 572 bp;

Kir2.3
Forward AAGGAGGAGCTGGAGTCAGAGGA,
Reverse ACTCAAGCATCCGGATAATGCCTG,
yielding a PCR product of 430 bp (Mermelstein *et al*., 1998).

The efficiency of these probes was demonstrated by their ability to detect Kir2.1, Kir2.2 and Kir2.3 subunits in RT-PCR from 10 pg of whole-brain total RNA (data not shown).

Results

The CIRK in cerebellar granule cells

In the present recordings performed at P19–22, a CIRK could be activated in 45.9% of recorded granule cells (45/98) by hyperpolarizing voltage pulses from the holding potential of −40 mV (Fig. 1A) as previously described (D'Angelo *et al*., 1995 in the rat; Rossi *et al*., 1998 in mice; Mathie *et al*., 2003). The CIRK currents were Ba^{2+}-sensitive (Rossi *et al*., 1998) and could be separated from leakage by subtraction of traces recorded in control solution and after 1 mM Ba^{2+} application. The CIRK current showed fast activation and attained steady-state in 1–2 ms. These properties were similar in WCR and PPR, which prevents cytoplasmic changes caused by cytoplasm washout by the patch-pipette (Horn & Marty, 1988).

The amplitude and voltage dependence of the CIRK current were investigated by fitting the *I–V* curves generated by depolarizing voltage-ramps with Eqn 1 (Fig. 1B). In the WCR configuration, curve fitting yielded half-activation potential $V_{1/2} = -91.2 \pm 1.5$ mV, voltage dependence of activation $k = 7.8 \pm 0.4$/mV and maximum conductance $G_{IR} = 0.86 \pm 0.1$ nS ($n = 35$ for all parameters). The reversal potential for potassium ions, $E_K = -85.7$ mV, was calculated from intra- and extracellular K^+ ionic activities (see Materials and methods for details). Leakage parameters were: $G_L = 0.66 \pm 0.04$ nS and $E_L = -52.4 \pm 2.1$ mV. The average activation curve of the CIRK current reconstructed using Eqn 2 is illustrated in Fig. 1C. The properties of the CIRK current were also evaluated using the PPR configuration (Fig. 1A). Fitting of *I–V* relationships obtained from voltage-ramps with Eqn 1 yielded CIRK and leakage parameters $V_{1/2} = -87.8 \pm 1.8$ mV, $k = 9.3 \pm 0.7$/mV, $G_{IR} = 0.9 \pm 0.2$ nS, $E_K = -85.7$ mV, G_L 0.43 ± 0.1 nS and $E_L = -35.1 \pm 4.4$ mV ($n = 10$ for all parameters). These parameters were not significantly different from those obtained in WCR. Given a cell membrane capacitance of 3.5 ± 0.3 pF ($n = 40$; see Materials and methods), the CIRK conductance was 245.7 ± 18.7 pS/pF ($n = 35$) in WCR and 257.1 ± 31.3 pS/pF ($n = 10$) in PPR, the two values being non-significantly different ($P = 0.45$, unpaired *t*-test). Therefore, most of the subsequent experiments, for the possibility of controlling the cytoplasmic ionic composition, of injecting intracellularly active compounds and of sampling the cytoplasm for RT-PCR, were performed in WCR. It should be noted that the biophysical properties for the rat CIRK current, including fast activation and strong rectification, were similar to those previously reported in mice (Rossi *et al*., 1998).

As previously reported in different preparations (e.g. Inoue & Imanaga, 1995), the CIRK current showed a tendency to run-down during the WCR. G_{IR} decreased by $23.5 \pm 3.0\%$ ($n = 11$) during the first 4 min after establishing the WCR configuration, thereafter CIRK tended to stabilize with just $14.0 \pm 7.6\%$ ($n = 11$) decrease in the next 10 min. Therefore, in order to allow comparison of various experimental conditions, subsequent measurements were normalized to G_{IR} measured 5 min after the beginning of recording (see Fig. 3B below).

Co-expression of Kir2 channels and $GABA_B$ receptors in single granule cells

In situ hybridization and immunohistochemistry have revealed high levels of Kir2.2 (Horio *et al*., 1996; Karschin *et al*., 1996) and a weaker signal for $GABA_B$ receptors subunits (Ige *et al*., 2000; Liang *et al*., 2000) in the cerebellum granular layer. Moreover, Kir2 transcripts were observed with a punctate pattern both in glia and neurons of the granular layer (Leonoudakis *et al*., 2001, 2004). It was, however, unknown whether Kir2 channels: (i) were correlated with the CIRK current; and (ii) were co-localized with $GABA_B$ receptors in single granule cells.

$GABA_B$ receptors comprise R1 and R2 subunits, and Kir2 channels include three main subtypes (Kir2.1, Kir2.2 and Kir2.3), which assemble in homo- or hetero-multimers to form functional channels. We have therefore investigated the localization of the corresponding mRNA at the level of single cerebellar granule cells using single-cell RT-PCR. The expression of transcripts coding for $GABA_BR1$ and $GABA_BR2$ receptor subunits and inwardly rectifying K^+ channels Kir2.1, Kir2.2 and Kir2.3 was examined in 13 visually identified cerebellar granule cells. To limit the number of cells with poor

retrieval of RT-PCR, we used only the results from 11 neurons showing the presence of transcripts coding for $GABA_A$ receptor α6-subunit, which is specifically expressed in cerebellar granule cells (Kato, 1990). A pair of primers located on two different exons was used to strengthen this positive control. The co-localization of $GABA_B$ receptor subunits and Kir channel α-subunits was demonstrated in four neurons (Fig. 2A). The percentage of $GABA_B$/Kir2 co-expression (36.4%) was similar to that of CIRK current expression (45.9%) in age-matched controls (P19–20). Kir channel subunits were either Kir2.1 or Kir2.2, while Kir2.3 was never observed.

In two of the four granule cells positive for Kir2 mRNA, electrophysiological recordings performed before withdrawing the cytoplasm revealed a CIRK current (G_{IR} > 0.4 nS) (Fig. 2B). Of the remaining seven cells, which did not show Kir2 mRNA expression, two showed a sizeable CIRK current while the other five did not. There was therefore a correlation between expression of mRNA for Kir2 channels, $GABA_B$ receptors and CIRK current, although this was not univocal, as further considered in the Discussion.

$GABA_B$ receptor-mediated inhibition of CIRK current

The functional coupling between $GABA_B$ and Kir2 channels was investigated by applying the $GABA_B$ receptor agonist, 30 μM baclofen. At the end of 10 min of baclofen perfusion in WCR, we observed a marked CIRK current decrease by 83.5 ± 5.5% (n = 19) (Fig. 3A and B; see Table 1 for statistical data). In order to rule out that washout of cytoplasmic constituents might be responsible for the effect, these experiments were replicated in PPR. In PPR, the CIRK current decreased by 70.8 ± 19.8% (n = 5). The decrease in CIRK current was statistically significant both for WCR and PPR, while the leakage current estimated from curve fitting in the same experiments did not show significant changes (the data and statistical tests are summarized in Table 1). In order to account for the effect of run-down, the WCR results have also been compared with normalized time-matched controls (same data as in Fig. 3B), still revealing a statistically significant decrease of the CIRK current following baclofen perfusion ($P < 1.8 \times 10^{-5}$, unpaired t-test).

The specificity of baclofen action was verified by preincubating slices for at least 30 min with 50 μM CGP35348, a selective $GABA_B$ receptor antagonist (Fig. 3A and B). In these recordings, during 10 min perfusion of baclofen +50 μM CGP35348, the CIRK current decreased by just 20.0 ± 2.0% (n = 4), a value that was not statistically different from time-matched controls (P = 0.46, unpaired t-test). These results therefore indicate that CIRK current inhibition by baclofen is mediated through $GABA_B$ receptors.

Because curve fitting yielded a change in CIRK without changes in leakage conductance (Table 1), the holding current could be taken as a further element to assess recording stability. The holding current recorded at −120 mV, where CIRK is activated, showed modest changes in control but showed a decrease when 30 μM baclofen was perfused (Fig. 3C). It should be noted that the effect of baclofen is smaller than in Fig. 3B because leakage was not subtracted in this case.

The effect of 30 μM baclofen was also observed following a short, 1-min perfusion. In this case, the CIRK current continued to decrease after cessation of perfusion until being reduced by 57.4 ± 4.6% (n = 7; $P < 0.0005$ unpaired t-test vs. normalized time-matched controls) after 8 min (Fig. 3B). Although washout with control solution was continued for up to 60 min in three cases, no reversal of baclofen effect was observed. Despite the prolonged washout, we could not totally exclude that persistence of baclofen within the slice was responsible for the persistent CIRK inhibition. We therefore performed very short perfusions (10–20 s) immediately followed by washout taking care of patching superficial granule cells and positioning the perfusion pipette near (< 100 μM) the recorded cell. In these experiments baclofen caused a rapid 81 ± 0.1% (n = 5) inhibition followed by partial recovery to 55.7 ± 2.7% (n = 5) of control upon washing with control solution (Fig. 4A and B). This value was still significantly smaller than time-matched controls ($P < 1 \times 10^{-8}$, unpaired t-test).

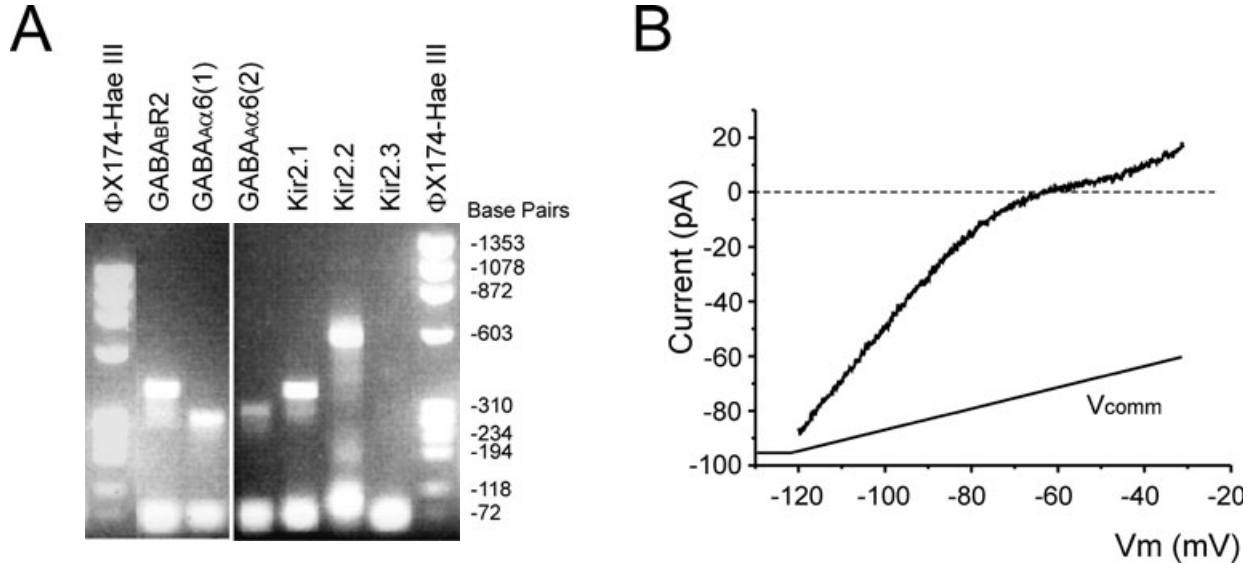

FIG. 2. Co-localization of γ-aminobutyric acid $(GABA)_B$ receptors and Kir2 channels in a granule cell showing inward rectifier current. (A) The agarose gel shows the presence of transcripts coding for the $GABA_BR2$ receptor subunit and for inwardly rectifying K^+ channels Kir2.1 and Kir2.2 in a cerebellar granule cell. Note the double positive control with two different $GABA_A$ α6 primers, and negativity to Kir2.3. Control molecular weight of ΦX174 DNA-Hae III digest in base-pairs (bp) to be confronted with: $GABA_BR2$, 401 bp; $GABA_ARA6$ Forward1, 300 bp; $GABA_ARA6$ Forward2, 300 bp; Kir2.1, 359 bp; Kir2.2, 572 bp; Kir2.3, 430 bp. (B) The corresponding membrane current recorded in voltage-clamp using a voltage-ramp from −120 to −30 mV (indicated as V_{comm}). Note the downward curvature of the I–V relationship denoting CIRK. Unlike elsewhere in the paper, no leak subtraction was used on these traces.

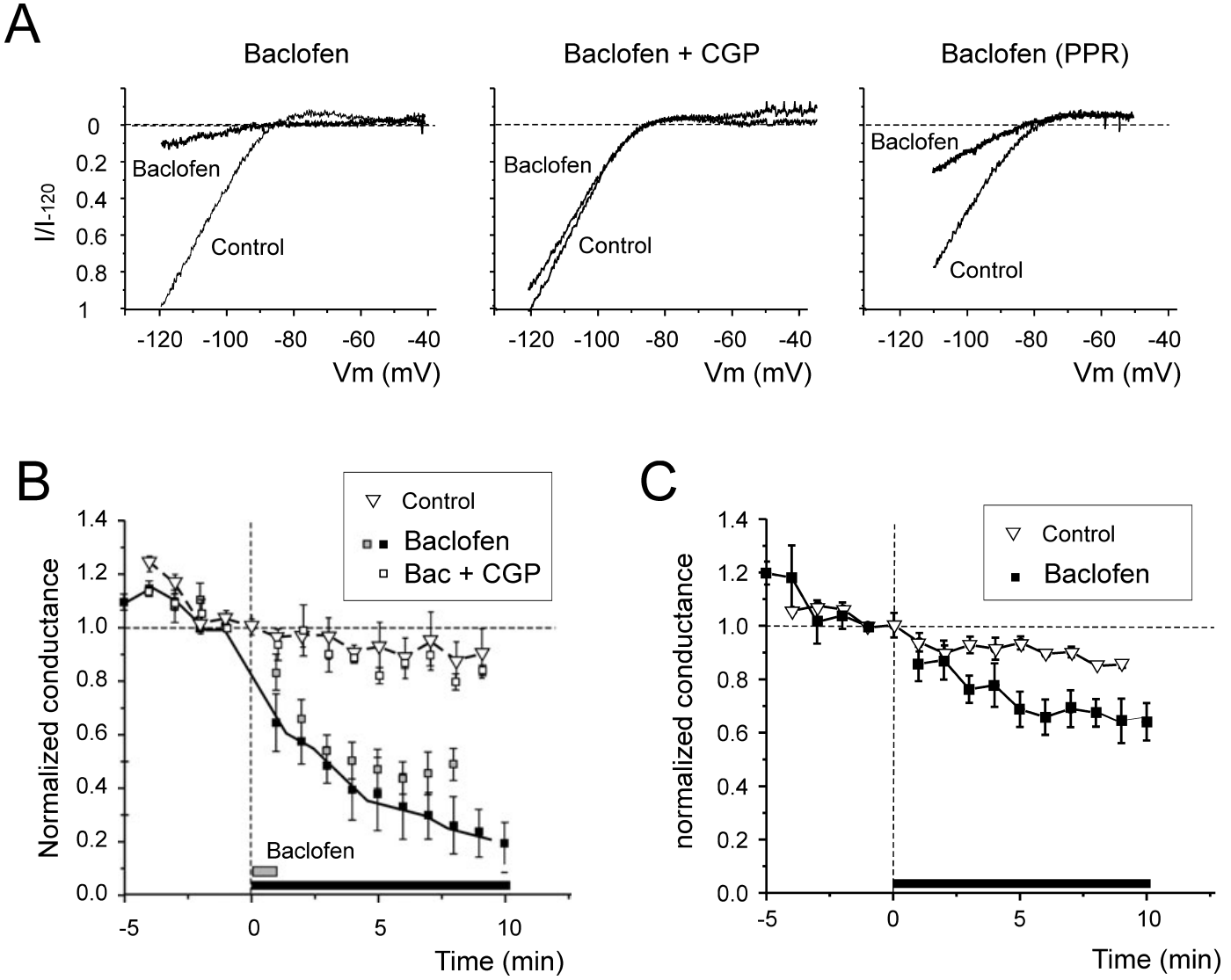

FIG. 3. Baclofen perfusion causes CIRK current inhibition. (A) CIRK currents elicited in WCR by a voltage-ramp in control (thin line) and after (thick line) 30 μM baclofen application in naïve slices (left panel), and in slices preincubated with 50 μM CGP35348 (middle panel). Baclofen inhibition in a PPR recording is shown in the right panel. (B) Average normalized time course of CIRK currents in various experimental conditions. At time 0, baclofen was perfused in control slices for the time indicated by the black bar ($n = 19$) and grey bar ($n = 7$). Baclofen was also perfused in CGP35348-preincubated slices for the time indicated by the black bar ($n = 4$). Baclofen inhibited CIRK only in the absence of CGP35348. Baclofen action is also compared with time-matched controls in WCR. Current amplitude was measured at −120 mV and normalized to the initial value. In this and in the following figures, CIRK currents are shown after leakage subtraction and are normalized to the value measured at −120 mV. (C) Holding current at −120 mV in control and after baclofen application. Same experiments as in (B). The two datasets indicate control condition and baclofen application.

TABLE 1. Conductance changes following baclofen application and synaptic stimulation

	Baclofen application (30 μM)				Synaptic stimulation (25 Hz)			
Conductance	(*n*)	Control	Baclofen	*P*-value	(*n*)	Control	Stimulation	*P*-value
G_{IR} (nS)								
WCR	(19)	1.47 ± 0.26	0.30 ± 0.43	< 0.0001	(5)	0.82 ± 0.16	0.16 ± 0.09	< 0.005
PPR	(5)	1.20 ± 0.14	0.41 ± 0.04	< 0.01	(3)	0.96 ± 0.10	0.15 ± 0.07	< 0.001
G_L (nS)								
WCR	(19)	0.66 ± 0.04	0.63 ± 0.26	0.60	(5)	0.65 ± 0.07	0.52 ± 0.04	0.34
PPR	(5)	0.51 ± 0.08	0.59 ± 0.08	0.63	(3)	0.67 ± 0.02	0.56 ± 0.02	0.1

Data were obtained using Eqn 1 to fit currents generated by voltage-ramps both in WCR and PPR. Currents were recorded in control and 8 min after commencing 30 μM baclofen application or after delivering the 25 Hz train of synaptic stimuli. Whereas G_{IR} decreases significantly, G_L remains almost unchanged. The statistical significance of comparisons is reported (paired *t*-test). Biophysical parameters of the CIRK current were statistically indistinguishable before and after application of baclofen or synaptic stimulation (data not shown). PPR, perforated-patch recording; WCR, whole-cell recording.

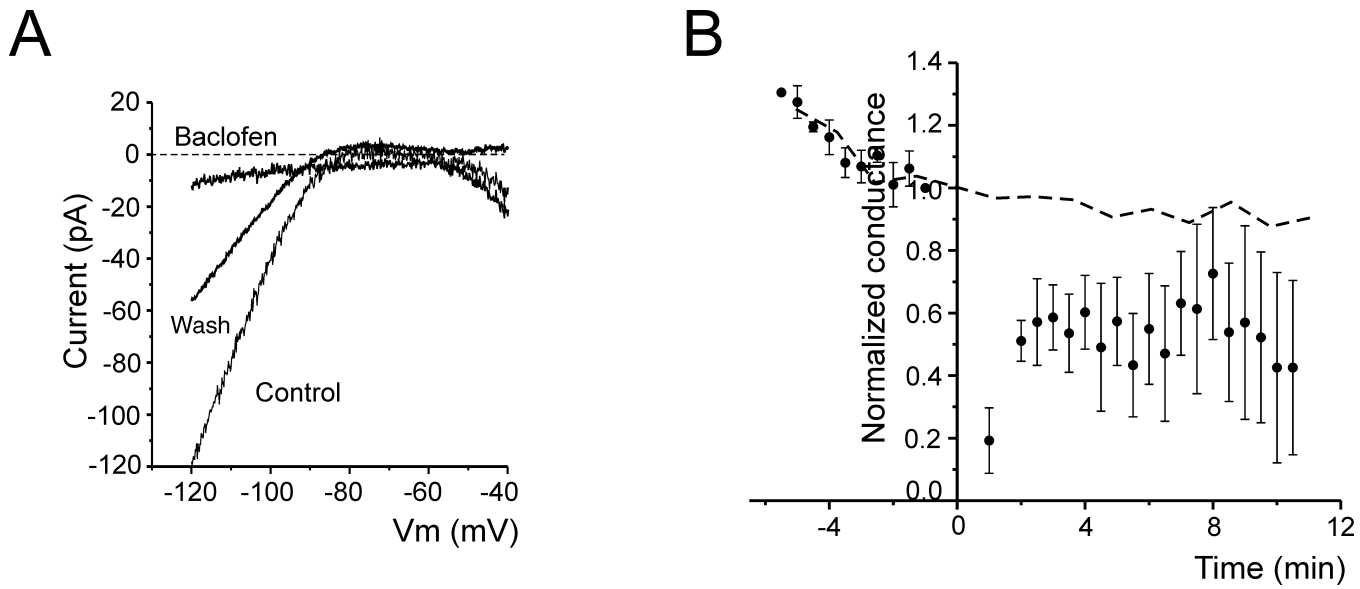

FIG. 4. The effect of baclofen perfusion is graded in amplitude and partially reversible. (A) Averaged voltage-ramp in control, 1 min after 30 μM baclofen perfusion, and during washout with control solution. Note partial recovery of the CIRK current with washing. (B) Averaged normalized time course of CIRK currents in short baclofen perfusion experiments. Local application of baclofen was started at time 0 and lasted for 20 s (arrowhead). The time course of control CIRK–current amplitude is replotted from Fig. 3B (broken line) for comparison.

In summary, all the granule cells expressing CIRK and tested for baclofen action showed a CIRK reduction (36/36). CIRK current inhibition appears therefore as a robust process, allowing further pharmacological and functional characterization of the inhibitory effect.

Cellular mechanisms of CIRK current inhibition by $GABA_B$ receptors

Modulation of the CIRK current has been reported in neuronal (Takano *et al*., 1995) and non-neuronal cells (Inoue & Imanaga, 1995; Kamouchi *et al*., 1997). In particular, Kir2.1 and Kir2.2 channels are regulated through a G-protein-dependent cascade involving processes of protein phosphorylation/dephosphorylation. Figure 5 illustrates the basic mechanisms of CIRK current regulation through $GABA_B$ receptors.

The possible involvement of G-proteins was tested by using the non-hydrolysable G-protein activator GTPγS (100 μM) in the patch-pipette. After obtaining the whole-cell configuration, CIRK current rapidly decreased reaching 75.2 ± 15.3% ($n = 5$; $P < 0.0015$, unpaired *t*-test vs. normalized time-matched controls) block in 8 min. The mechanism appeared therefore to be G-protein sensitive. Interestingly, in other neurons, like retinal ganglion cells (Chen *et al*., 2004), hippocampal CA1 pyramidal cells (Chen & Johnston, 2005) and nucleus basalis neurons (Hoang *et al*., 2004), GTPγS enhances a tonically active inward rectifier current, which is, however, related to channels different from Kir2 (Kir3 or KirNB). The potential presence of Kir3 channels in granule cells is further addressed in Fig. 8 and in the Discussion.

In order to test the nature of G-proteins involved in the $GABA_B$ pathway, we incubated slices overnight with 5 μg/mL PTX in a continuously oxygenated chamber. The same PTX concentration was also added to the patch-pipette solution. PTX catalyses ADP-ribosylation of the α-subunit of G_i, preventing GDP displacement by GTP and blocking downstream inhibition of adenylate cyclase. In these experiments, 8 min of baclofen perfusion could still block CIRK current by 89.0 ± 5.6% ($n = 4$; $P < 0.001$; unpaired *t*-test vs. normalized time-matched controls), ruling out the involvement of a PTX-sensitive mechanism. It should be noted that the main granule cell membrane properties after overnight incubation were similar to those recorded in fresh slices (Fig. 5A, inset). (i) During hyperpolarizing voltage-clamp protocols, the CIRK current was observed in 45% (5/11) of granule cells with $G_{IR} = 1.68 \pm 0.3$ nS ($n = 5$; not significantly different from WCR data in Table 1). (ii) During depolarizing voltage-clamp protocols, all cells showed inward and outward currents. At the test potential of −20 mV (PTX-incubated vs. control), the peak inward current was −314 ± 21.5 pA ($n = 11$) vs. −294.4 ± 48.6 pA ($n = 7$), the transient outward current was 129 ± 12.3 pA vs. 165 ± 24.8 pA, and the steady-state outward current was 30.1 ± 5.4 pA vs. 27.2 ± 4.6 pA. None of the measurements was statistically different from controls. (iii) Membrane capacitance was 4.1 ± 0.2 pF ($n = 11$; NS vs. WCR data in Materials and methods).

The potential regulation of the balance of phosphorylation downstream of G-protein activation was assessed by intracellular perfusion through the patch-pipette of okadaic acid (1 μM), a protein phosphatase inhibitor that inhibits CIRK modulation in chromaffin and arterial pulmonary endothelial cells (Inoue & Imanaga, 1995; Kamouchi *et al*., 1997). After 8 min of 30 μM baclofen application, the CIRK current decreased by 11.4 ± 12.1% ($n = 9$; $P = 0.85$, unpaired *t*-test vs. normalized time-matched controls). Thus, okadaic acid prevented baclofen action.

These results (summarized in Fig. 5C) indicate inhibitory control of CIRK channels by $GABA_B$ receptors through a PTX-insensitive G-protein-mediated pathway regulating protein phosphorylation at some critical steps.

Repetitive inhibitory synaptic activity causes CIRK current inhibition

In order to investigate the functional implications of $GABA_B$ receptor-mediated inhibition of CIRK currents and to determine whether the

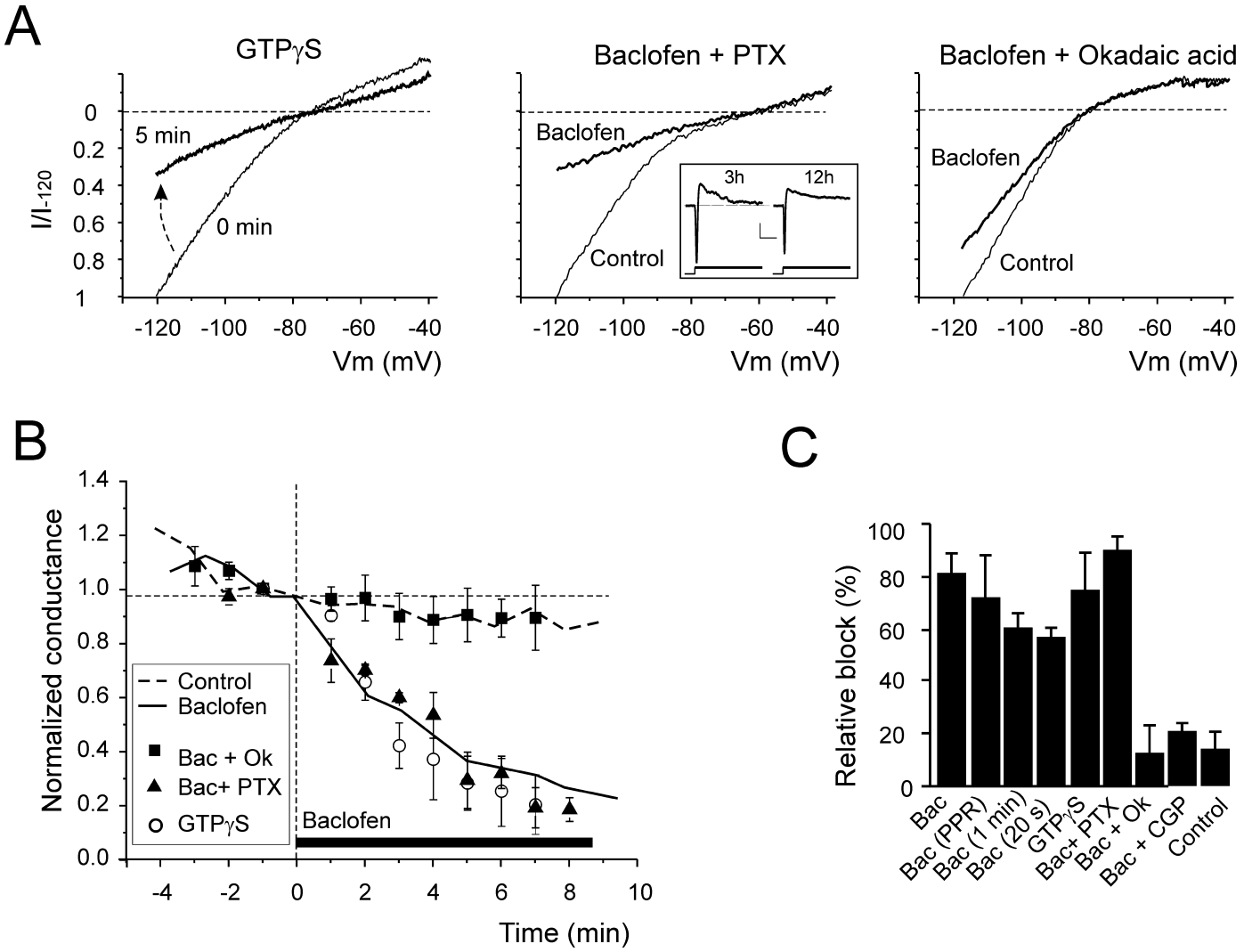

FIG. 5. Mechanism of CIRK current inhibition. (A) CIRK currents were elicited by voltage-ramps. Left, GTPγS (100 μM) was added to the patch-pipette solution. Note inhibition of inward rectification, as indicated by the arrow. Middle, baclofen was perfused in slices preincubated overnight with pertussis toxin (PTX, 5 μg/mL). The inset shows whole-cell voltage-dependent currents elicited with a depolarizing pulse from −80 mV to −10 mV at 3 h and 12 h after PTX incubation. Both the inward and outward components are visible. Right, baclofen was perfused in the presence of okadaic acid (1 μM) in the patch-pipette. Tracings are taken before and 8 min after starting baclofen application (see B), except in the case of GTPγS, in which no baclofen was applied and the effect of the drug was evaluated 5 min after commencing the recording. (B) Average normalized time course of CIRK current in the experimental conditions exemplified in (A). Local application of baclofen was started at 0 and continued for the time indicated by the black bar. The control and baclofen time course are replotted from Fig. 3B. (C) Histogram summarizing the relative CIRK current change in different experimental conditions: 8-min 30 μM baclofen in WCR ($n = 19$); 8-min 30 μM baclofen in PPR ($n = 5$); 1-min 30 μM baclofen in WCR ($n = 19$); 20-s 30 μM baclofen in WCR ($n = 19$); 5-min 100 μM GTPγS in the patch-pipette ($n = 5$); 8-min 30 μM baclofen + 5 μg/mL PTX overnight ($n = 4$); 8-min 30 μM baclofen + 1 μM okadaic acid in the patch-pipette ($n = 9$); 8-min 30 μM baclofen + 50 μM CGP35348 ($n = 4$); time control in WCR ($n = 11$).

effect could be observed with physiologically meaningful stimulation, the inward rectifier current was measured in response to various activity patterns in Golgi cell axons. Cerebellar granule cells receive their inhibitory input from GABAergic synapses provided by Golgi cells. Stimulation experiments have been performed in the presence of blockers for α-amino-3-hydroxy-5-methyl-4-isoxazolepropionic acid (AMPA) (10 μM CNQX), *N*-methyl-D-aspartate (NMDA) (100 μM APV +50 μM 7-Cl-kyn) and metabotropic (500 μM MCPG) glutamate receptors in order to prevent potential effects caused by mossy fibre activation on granule cells (D'Angelo *et al.*, 1995, 1999) and Golgi cell presynaptic terminals (Mitchell & Silver, 2000). By analogy with pharmacological experiments, in which the effect developed after baclofen application, we monitored the CIRK current following application of specific synaptic stimulation patterns. In these recordings, after controlling stimulation efficacy using low-frequency impulses (0.1 Hz), IPSCs were blocked with bicuculline (Fig. 6B).

Because Golgi cells are pacemaker neurons with autorhythmic activity at about 4 Hz at room temperature *in vitro* (Dieudonne, 1998; Forti, Cesana, Mapelli and D'Angelo, unpublished observation), we first tested the effect of a 4 Hz continuous stimulation on CIRK current amplitude (Fig. 6A and B). CIRK current reduction (18.0 ± 6.1% after 8 min of stimulation, $n = 5$) was not statistically different from run-down in control experiments ($P = 0.7$; unpaired *t*-test vs. normalized time-matched controls). A second stimulus pattern was selected by considering that Golgi cells *in vivo* can undergo protracted periods of sustained discharge at about 25 Hz (Edgley & Lidierth, 1987; Vos *et al.*, 1999a). Thus, in a series of recordings a 25 Hz train was delivered for 2 min. At the end of

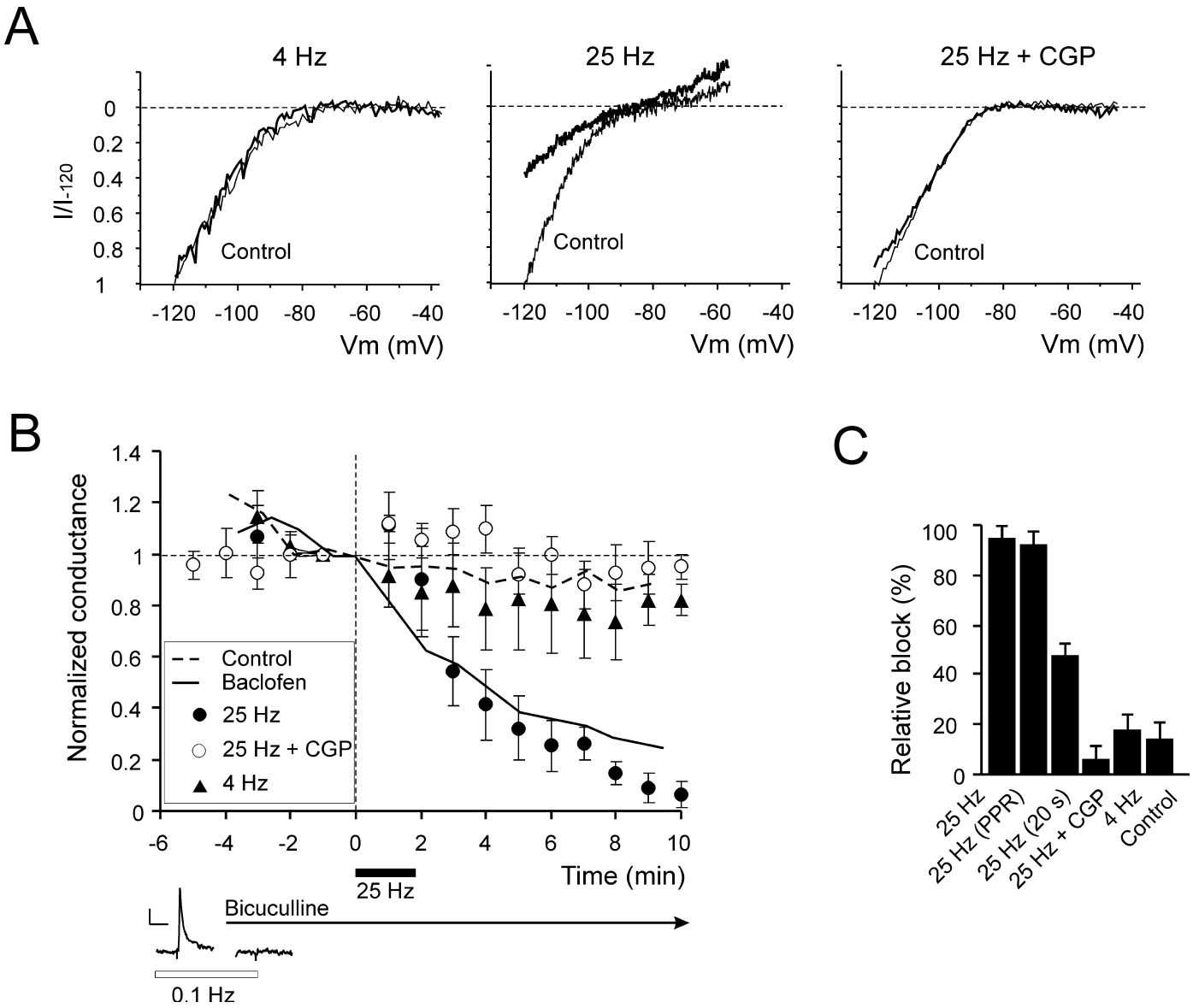

FIG. 6. Golgi cell axon stimulation causes CIRK current inhibition. These recordings were performed in the presence of 10 μM CNQX, 100 μM APV, 50 μM 7-Cl-kyn and 500 μM MCPG. (A) CIRK currents elicited by voltage-ramps protocol in control (thin line) and after Golgi cell axon stimulation (thick line). Left, 4 Hz continuous. Middle, 25 Hz for 2 min. Right, 25 Hz for 2 min in slices preincubated and perfused with CGP35348. (B) Average normalized time course of CIRK current amplitude measured at −120 mV in the experimental conditions exemplified in (A). Golgi cell axon stimulation was commenced at 0 and continued for the rest of the recording at 4 Hz or for 2 min at 25 Hz (black bar). The control and baclofen time course are replotted from Fig. 3B. Bottom: IPSCs recorded at 0.1 Hz to demonstrate the efficiency of stimulation were then blocked by 30 μM bicuculline. (C) Mean percent block of CIRK current 8 min after different stimulation paradigms including 2-min 25 Hz stimulation in WCR ($n = 5$) and in PPR ($n = 3$), 2-min 25 Hz stimulation + 50 μM CGP35348 ($n = 6$), continuous stimulation at 4 Hz ($n = 5$), time control in WCR ($n = 11$).

stimulation the CIRK current was reduced by 45.6 ± 13.5% ($n = 5$; Fig. 6A and B). CIRK current then continued to decrease until being reduced by 95.0 ± 4.3% ($n = 5$) 8 min after the beginning of stimulation (Fig. 6C; Table 1). The time course of the change was similar to that determined by baclofen application. Similar results were observed also using 25 Hz stimulation in perforated-patch recordings, with a reduction of 91.7 ± 6.9% ($n = 3$) 8 min after the beginning of stimulation (not shown). Neither in WCR nor PPR did leakage show any noticeable change (Table 1). In order to account for the effect of run-down, the WCR results have also been compared with normalized time-matched controls, still revealing a statistically significant decrease of the CIRK current following stimulation ($P < 0.3 \times 10^{-10}$, unpaired *t*-test).

The dependence of the effect on the duration of stimulation was tested by applying a short train of 25 Hz stimuli lasting just 20 s. In this case, CIRK current reduction reached an intermediate level of 52.9 ± 4.5% ($n = 5$; $P < 0.0001$, unpaired *t*-test vs. normalized time-matched controls) 8 min after the beginning of stimulation (see Fig. 5C). The dependence of the effect on $GABA_B$ receptors was tested by preincubating the slices for (at least) 30 min with 50 μM CGP35348. As in previous recordings, a 25 Hz stimulation was applied for 2 min. This reduced the CIRK current by just 5.1 ± 5.3% ($n = 6$; $P = 0.1$, unpaired *t*-test vs. normalized time-matched controls). The mean percent block of CIRK current in the different stimulation conditions is reported in Fig. 6C.

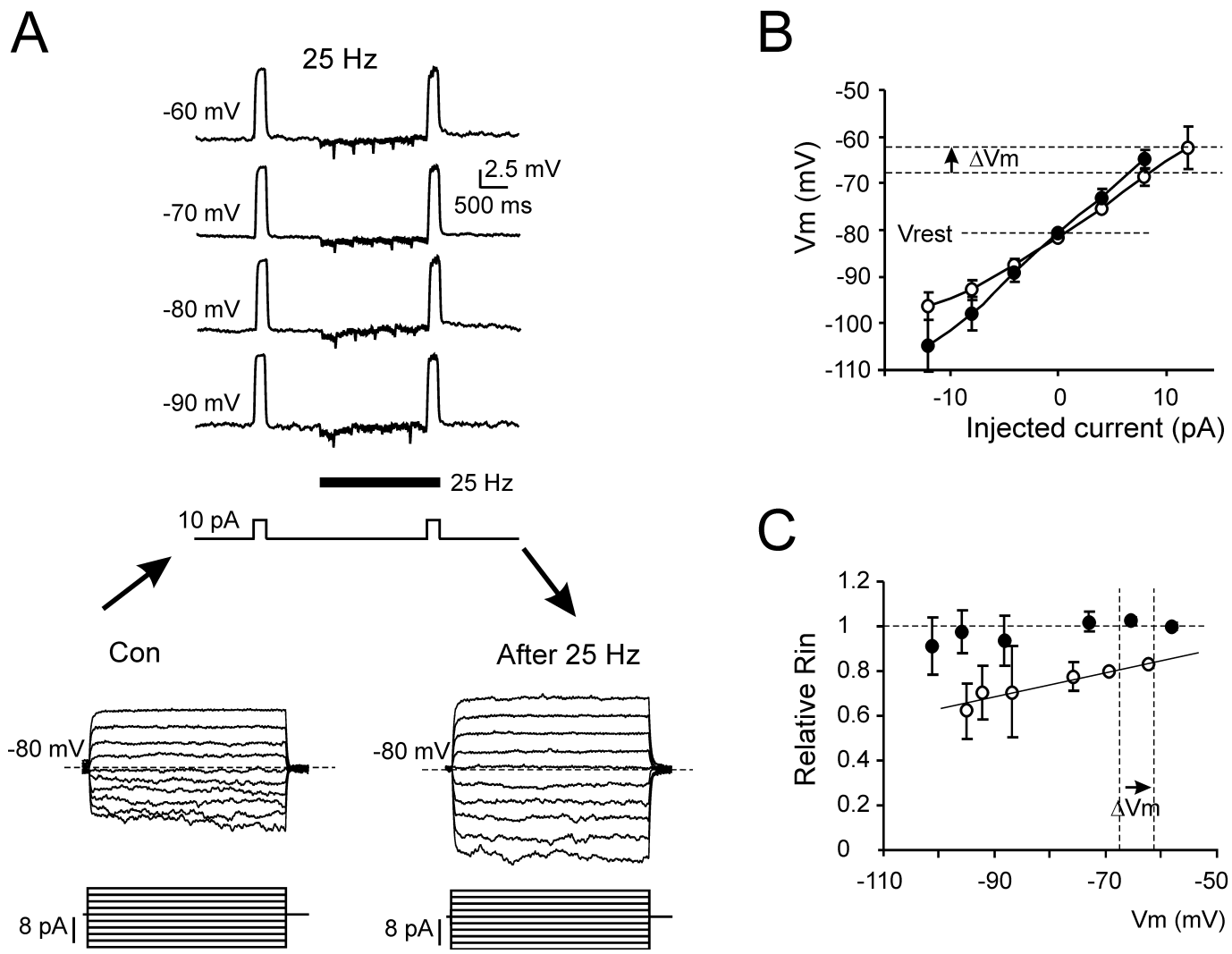

FIG. 7. Subthreshold changes following high-frequency Golgi cell axon stimulation. (A) Responses to synaptic stimulation at 25 Hz for 2.2 s. Stimulus trains were delivered every 10 s for 2 min from different membrane potentials comprised between −80 mV and −50 V. Test current pulses (+4 pA) were injected before and during synaptic stimulation to measure input resistance. No changes in membrane potential or input resistance were observed during the trains. Granule cell responses to current injection (bottom tracings 2 pA/step, top tracing 10 pA) were evoked from −80 mV both before and 5 min after terminating the synaptic stimulus trains. Note that granule cell inward rectification is strongly reduced after the trains. (B) Average plot ($n = 5$) for steady-state responses to step current injection before (○) and after 25 Hz stimulation (●). Note that the slope of the *V–I* relationship is increased at low potentials. The resting membrane potential is shifted toward depolarized values (dotted lines and arrow) following 25 Hz stimulation. (C) The input resistance (R_{in}) of the same granule cells of (A) and (B) is shown normalized to the control value at −58 mV. In control (○), R_{in} shows a significant decrease with membrane potential ($n = 5$; $R_2 = 0.89$; $P < 0.01$). After 25 Hz stimulation (●), R_{in} becomes nearly constant. It should be noted that there is a sizeable divergence of values measured before and after stimulation in the subthreshold region, suggesting that CIRK takes part in regulating synaptic integration.

Effects of repetitive inhibitory synaptic activity on subthreshold intrinsic excitability

The effect of a CIRK current reduction on subthreshold Golgi cell responses is shown in Fig. 7. In 10 recordings, after measuring the IPSCs to check the efficiency of synaptic stimulation, $GABA_A$ receptors were blocked by 30 μM bicuculline, and granule cell membrane potential and input resistance were monitored in current-clamp. In 50% of cases the granule cells showed inward rectification in the negative membrane potential range (D'Angelo *et al.*, 1995; Rossi *et al.*, 1998). In these cells, during repetitive stimulation (2.2 s at 25 Hz) no appreciable membrane potential changes were observed from resting potentials maintained by constant current injection between −80 mV and −50 mV (0.5 ± 0.04 mV difference from baseline; $n = 10$; NS), i.e. in a range that would allow detection of changes in K^+ currents. Moreover, the cell input resistance, measured from the response to small depolarizing current pulses, did not change (1.4 ± 0.2 GΩ at the beginning and 1.5 ± 0.4 GΩ at the end of stimulus trains; $n = 10$; NS). These results ruled out any regulation of granule cell electroresponsiveness *during* repetitive stimulation by subthreshold-activating conductances potentially coupled to $GABA_B$ receptors.

A further analysis was restricted to the five cells showing inward rectification. Following 12–30 train repetitions, inward rectification was markedly reduced, as expected from voltage-clamp recordings (Fig. 7A and B). The subthreshold *I–V* relationship became steeper after repetitive stimulation, and this modification increased granule cell input resistance by nearly 20% between −60 mV and −70 mV (Fig. 7C). Moreover, resting membrane potential changed from −68.6 ± 3.3 mV to −62.2 ± 3.4 mV ($n = 5$; $P < 0.02$, paired *t*-test).

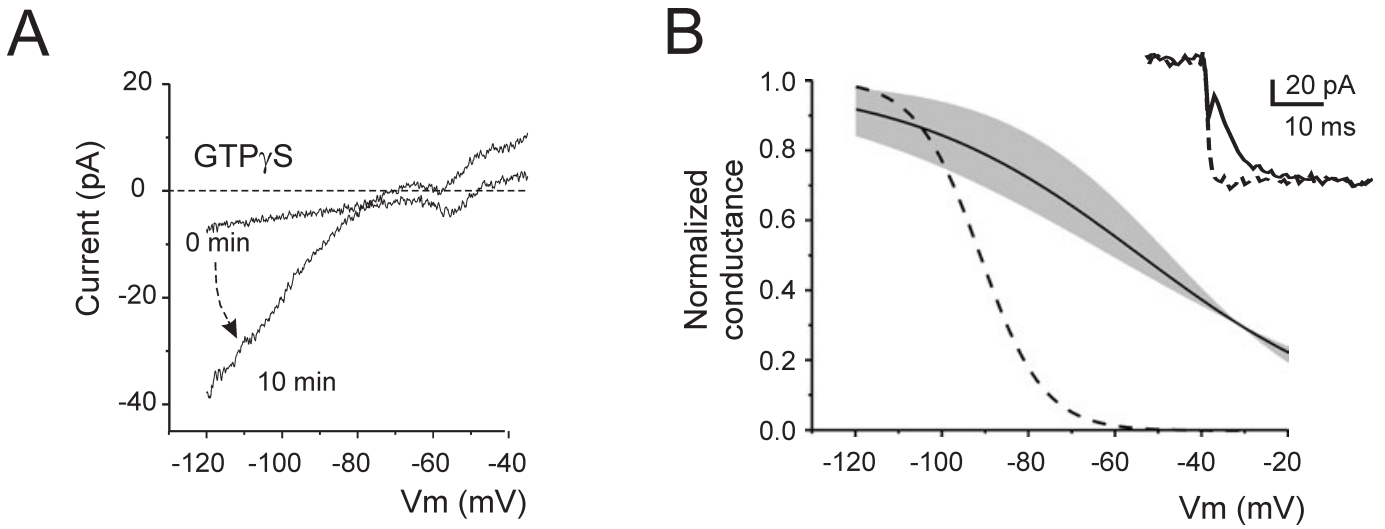

FIG. 8. GIRK currents in granule cells. The figure shows the effect of 100 μM GTPγS in the patch-pipette. (A) Example of recordings taken at the beginning and after 8 min from the beginning of the whole-cell recording. Note the development of inward rectification, as indicated by the arrow. (B) Steady-state activation curve for the GIRK current. Averaged normalized conductance curve ($n = 8$) constructed by Eqn 2. The shaded area indicates the MSE of curve fitting obtained from individual experiments. The CIRK activation curve is replotted from Fig. 1C for comparison (dashed line). The inset shows the activation kinetics in GIRK and CIRK (dashed line) currents recorded at −120 mV, which have been scaled to the same plateau amplitude.

Therefore, CIRK reduction brought about changes tending to enhance excitability in a membrane potential region relevant to granule cell functioning. An associated reduction in spike threshold (data not shown), which may suggest additional modulatory processes determined by repetitive stimulation, prevented a further analysis of the functional consequences of CIRK current inhibition on granule cell firing.

Granule cells expressing GIRK rather than CIRK current

A puzzling aspect of our finding is that, although Kir3 channels have been reported in the cerebellum granular layer at mature developmental stages (Karschin *et al*., 1996; Liao *et al*., 1996), no clear evidence for the corresponding GIRK current emerged. We therefore performed a series of whole-cell recordings with GTPγS in the patch-pipette to detect whether GIRK could be observed in some cases. In some of these recordings (seven out of 15), as already documented in Fig. 4, we observed a CIRK current showing a marked time-dependent decrease. Conversely, in all the granule cells without CIRK at the beginning of recordings (eight out of 15), we observed a progressive growth of inward rectification (Fig. 8A). This GIRK current had weaker voltage dependence than CIRK. Fitting of *I–V* relationships obtained from voltage-ramps 8 min after commencing the whole-cell recording using Eqn 1 yielded GIRK and leakage parameters $V_{1/2} = -54.3 \pm 6.8$ mV, $k = 27.3 \pm 8.0$/mV, $G_{IR} = 1.3 \pm 0.2$ nS, $E_K = -85.7$ mV, $G_L = 1.0 \pm 0.2$ nS and $E_L = -32.7 \pm 7.4$ mV ($n = 8$). $V_{1/2}$, k and G_{IR} were significantly different from those of CIRK currents ($P < 0.01$ in all cases; unpaired *t*-test). Moreover, the currents attained 90% of steady-state amplitude in 10–20 ms at test potentials between −50 mV and −120 mV (Fig. 8B, inset). The granule cells without CIRK have therefore the potential to show functional GIRK activation.

Discussion

This paper shows that CIRK currents can be inhibited by activation of $GABA_B$ receptors at the Golgi cell–granule cell relay of the cerebellum. Following either baclofen application or appropriate patterns of synaptic stimulation, CIRK gradually decreased until reaching about 20% of its initial amplitude in 5–10 min. As a consequence, subthreshold neuronal excitability was enhanced. This observation contrasts with the more common finding of $GABA_B$ receptor-mediated enhancement of GIRK currents (Misgeld *et al*., 1995; Nicoll, 2004). The difference between CIRK- and GIRK-mediated responses extends to the IPSCs. GABAergic transmission in cerebellar granule cells evokes IPSCs uniquely determined by $GABA_A$ receptors (Rossi *et al*., 2003), while in neurons of the hippocampus and visual cortex IPSCs consist of an early $GABA_A$ Cl^--dependent component and a late $GABA_B$ K^+-dependent component mediated by GIRK channel activation (Connors *et al*., 1988; Dutar & Nicoll, 1988).

The specificity of CIRK inhibition through $GABA_B$ receptors was supported by the preventative action of the $GABA_B$ receptor antagonist CGP35348. CGP35348 similarly prevented CIRK inhibition caused by baclofen application and repetitive stimulation (see below). This observation suggests that synaptic stimulation activates the same receptors and transduction pathway causing the pharmacological effects. Because, during synaptic stimulation, CIRK inhibition was observed in the presence of $GABA_A$ receptor blockade, modulation of the tonic GABA current of granule cells (Brickley *et al*., 1996; Rossi *et al*., 2003) could be ruled out. Moreover, synaptic stimulation was performed in the presence of mGluR, NMDA and AMPA receptor blockers, preventing potential postsynaptic effects mediated by simultaneous activation of mossy fibres (Armano *et al*., 2000) or activation of presynaptic mGluR on Golgi cell terminals (Mitchell & Silver, 2000). We cannot, however, exclude that other neurotransmitters were co-released with GABA from the Golgi cell terminals contributing to the effect. Substance P and muscarine proved to inhibit CIRK in neurons of the central (Takano *et al*., 1995; Velimirovic *et al*., 1995) and peripheral (Wang & McKinnon, 1996) nervous system.

Either using baclofen or synaptic stimulation, CIRK current inhibition outlasted the presentation of the stimulus. On the one hand, the possibility that baclofen remained in the slice at a sufficient concentration to activate $GABA_B$ receptors even during washout

cannot be excluded, as partial reversibility of the effects was observed with brief and localized baclofen perfusion. On the other hand, the observation of CIRK inhibition using repetitive synaptic stimulation is in favour of a physiological mechanism protracting CIRK inhibition. Thus, it is possible that CIRK inhibition represents a long-lasting modulation or even a long-term change in intrinsic excitability (so-called non-synaptic plasticity), of which a few examples have been reported in neurons (Armano *et al*., 2000; Hansel *et al*., 2001; Debanne *et al*., 2003; Zhang & Linden, 2003).

Molecular substrates of the CIRK current in cerebellar granule cells

Single-cell RT-PCR revealed Kir2.2 α-subunit mRNA in granule cells, confirming previous findings with *in situ* hybridization and immunostaining (Karschin *et al*., 1996; Horio *et al*., 1996; Stonehouse *et al*., 1999; Leonoudakis *et al*., 2001, 2004), and also showed Kir2.1, which was not reported previously. Kir2 and CIRK current expression were correlated: 50% of granule cells co-expressed CIRK and Kir2, and 70% of granule cells without Kir2 mRNA did not show CIRK (the remaining 30%, showing CIRK but no Kir2, may reflect the inability of RT-PCR in revealing Kir2 due to the small size of granule cells and the correspondingly limited cytoplasm harvest). Thus, Kir2 was the most likely substrate for CIRK. The presence of Kir2 but not CIRK in some cells may reflect CIRK inhibition, e.g. through endogenous $GABA_B$ receptor activation.

Consistent with Kir2.1 and Kir2.2 channels reconstituted in expression systems (Dhamoon *et al*., 2004), CIRK currents showed fast kinetics and steep voltage dependence. Similar biophysical properties have been observed in other neurons (Takano *et al*., 1995; Velimirovic *et al*., 1995; Wang & McKinnon, 1996), chromaffin cells (Inoue & Imanaga, 1995), endothelial cells (Kamouchi *et al*., 1997) and cardiac myocytes (Dhamoon *et al*., 2004) expressing Kir.2 channels.

Kir3 channels generate GIRK currents in premigratory granule cells (Rossi *et al*., 1998) and in cultures from newborn pups (Slesinger *et al*., 1997). Here we show that GIRK currents can also be observed in postmigratory granule cells that do not have CIRK. Different from CIRK, GIRK currents showed weak voltage dependence and slow activation kinetics (as reported by Kofuji *et al*., 1996; Rossi *et al*., 1998). This observation is consistent with *in situ* hybridization and immunostaining, which revealed Kir3 mRNA and channels in the granular layer (Karschin *et al*., 1996; Liao *et al*., 1996). However, it is improbable that GIRK co-existed with CIRK, as the current remaining after inhibition (GTPγS intracellular perfusion, baclofen application or synaptic activation) maintained the biophysical properties of CIRK. It seems more probable that CIRK and GIRK are segregated in different granule cells, maybe reflecting different degrees of maturation or yet unknown mechanisms of regulation. High-resolution immunolabelling may be used to reveal whether Kir2 and Kir3 channels segregate in different granule cells. Another interesting issue is whether, as reported by Slesinger *et al*. (1997) in cell culture, GIRK currents in the granular layer *in situ* are also modulated by $GABA_B$ receptor activation.

Our results support the conclusion that constitutive inward rectification of cerebellar granule cells *in situ* is determined by CIRK rather than GIRK currents, and is therefore related to the expression of Kir2 rather than Kir3 channels. The constitutive inward rectification of granule cells differs therefore from tonic G-protein-mediated modulation of Kir3 channels reported in retinal ganglion cells (Chen *et al*., 2004) and in the dendrites of hippocampal CA1 pyramidal neurons (Chen & Johnston, 2005) or from activation of KirNB channels reported in cultured nucleus basalis neurons (Hoang *et al*., 2004).

Properties of the transduction pathway

Single-cell RT-PCR revealed $GABA_BR1$ and $GABA_BR2$ mRNA, in agreement with previous *in situ* hybridization experiments (Liang *et al*., 2000). In 36.4% of neurons, $GABA_B$ receptor subunits and Kir channel α-subunits were co-localized, providing the molecular substrate for functional coupling. The Golgi cell–granule cell synapses are located on the dendrites and are enwrapped within a glial sheet forming the cerebellar glomerulus and limiting neurotransmitter diffusion (Rossi *et al*., 2003). It is therefore probable that synaptically released GABA activates the $GABA_B$-Kir2 inhibitory mechanism within the glomerulus. Consistently, immunostaining reveals a dendritic localization of $GABA_B$ receptors (Ige *et al*., 2000) and Kir2.2 channels (Stonehouse *et al*., 1999). It should be noted that $GABA_B$ receptors are also present in the granule cell axon, the parallel fibre, where GABA released from molecular layer interneurons causes heterosynaptic depression of glutamate release through presynaptic $GABA_B$ receptor activation and Ca^{2+} channel modulation (Dittman & Regehr, 1997).

The coupling of Kir2 channels to membrane molecular complexes provides the substrate for channel regulation processes (Leonoudakis *et al*., 2001, 2004). An initial characterization of the transduction pathway has revealed that $GABA_B$ receptor-dependent CIRK modulation involves a PTX-insensitive G-protein and a cytoplasmic dephosphorylation process blocked by okadaic acid in the patch-pipette. A quite similar process was reported in endothelial cells (Kamouchi *et al*., 1997), and CIRK currents inhibited by GTPγS were also observed in chromaffin cells (Inoue & Imanaga, 1995). In nucleus basalis neurons, CIRK current inhibition is promoted by substance P and occurs through a PTX-insensitive G-protein but, unlike in granule cells, is prevented by phosphatases and enhanced by protein kinase C (Takano *et al*., 1995). The transduction pathway in granule cells may be further investigated by using different receptor agonists, by selective blockage of G-protein subtypes, and by using inhibitors of intracellular kinases (like protein kinase C or A) or phosphatases potentially involved in CIRK regulation.

Functional implications of CIRK current inhibition

CIRK inhibition depolarized the granule cell and increased input resistance in a membrane potential range (between −70 mV and −60 mV) compatible with subthreshold synaptic integration (Fig. 7B and C). Although this is expected to raise granule cell excitability in terms of spike output, the direct assessment of this effect is unpractical due to the potential action of $GABA_B$ receptors on multiple membrane channels (Misgeld *et al*., 1995; Nicoll, 2004). Further experimental work is needed to prove this hypothesis. The potential functional implications of CIRK inhibition descend from the properties of Golgi cell–granule cell interaction and the functional organization of the granular layer circuit. Golgi cells are pace-maker neurons beating at about 4 Hz in slices. It is interesting to note that, in order to induce CIRK inhibition, the axons had to be stimulated at 25 Hz, i.e. at a frequency higher than basal Golgi cell discharge. Because protracted activity at about 25 Hz has been observed in a fraction of Golgi cells *in vivo* (Edgley & Lidierth, 1987; Vos *et al*., 1999a), there could be regions in the cerebellum granular layer undergoing CIRK current inhibition.

The pro-excitatory action of CIRK current inhibition is puzzling for a GABAergic synapse. It is tempting to speculate that the increase in

granule cell excitability following $GABA_B$ receptor-mediated CIRK inhibition has an homeostatic significance (Turrigiano & Nelson, 2004), preventing excess inhibition of synaptic transmission along the mossy fibre pathway. Synaptic inhibition is supposed to provide a powerful mechanism to limit the number of active granule cells, a property called sparse coding (Marr, 1969). Although sparseness is thought to be important, an insufficient number of active granule cells would lead to information loss and degradation of mossy fibre representations (Schweighofer *et al*., 2000). Thus, CIRK inhibition through $GABA_B$ receptors may contribute to determine the appropriate balance in the number of granule cells activated by a given input.

Acknowledgements

We thank Dr M. Podda for participation in preliminary experiments, and D. Houtteman for expert technical assistance. This work was supported by projects of the European Community (CEREBELLUM QLG3-CT-2001-02256 and SPIKEFORCE IST-2001-35271), of MIUR and INFM of Italy to E.D., and by Fondation Médicale Reine Elisabeth (Belgium), Fond National de la Recherche Scientifique (Belgium), Action de Recherche Concertée (2002-07) to S.S. A.dK. is research Associate at the FNRS (Belgium).

Abbreviations

7-Cl-kyn, 7-chlorokinurenic acid; AMPA, α-amino-3-hydroxy-5-methyl-4-isoxazolepropionic acid; APV, D-2-amino-5-phosphonovaleric acid; CIRK, constitutive inward rectifier K^+-current; CNQX, 6-cyano-7-nitroquinoxaline-2,3-dione; GABA, γ-aminobutyric acid; GIRK, G-protein-dependent inward rectifier K^+-currents; IPSC, inhibitory postsynaptic current; MCPG, (+)-α-methyl-4-carboxyphenyl-glycine; NMDA, *N*-methyl-D-aspartate; PPR, perforated-patch recording; PTX, pertussis toxin; RT-PCR, reverse transcriptase-polymerase chain reaction; WCR, whole-cell recording.

References

Armano, S., Rossi, P., Taglietti, V. & D'Angelo, E. (2000) Long-term potentiation of intrinsic excitability at the mossy fiber–granule cell synapse of rat cerebellum. *J. Neurosci.*, **20**, 5208–5216.

Barthel, F., Kielnen, C., Demeneix, B.A., Feltz, P. & Loffler, J.Ph. (1996) GABAB receptors negatively regulate transcription in cerebellar granular neurons through cyclic AMP responsive element binding protein-dependent mechanisms. *Neuroscience*, **70**, 417–427.

Brickley, S.G., Cull-Candy, S.G. & Farrant, M. (1996) Development of a tonic form of synaptic inhibition in rat cerebellar granule cells resulting from persistent activation of $GABA_A$ receptors. *J. Physiol. (Lond.)*, **497**, 753–759.

Chandy, K.G. & Gutman, G.A. (1993) Nomenclature for mammalian potassium channel genes. *Trends Pharmacol. Sci.*, **14**, 434–439.

Chen, Y.-L., Huang, C.C. & Hsu, K.S. (2001) Time-dependent reversal of long-term potentiation by low-frequency stimulation at the hippocampal mossy-fiber-CA3 synapses. *J. Neurosci.*, **21**, 3705–3714.

Chen, X. & Johnston, D. (2005) Constitutively active G-protein-gated inwardly rectifying K+ channels in dendrites of hippocampal CA1 pyramidal neurons. *J. Neurosci.*, **25**, 3787–3792.

Chen, L., Yu, Y.C., Zhao, J.W. & Yang, X.L. (2004) Inwardly rectifying potassium channels in rat retinal ganglion cells. *Eur. J. Neurosci.*, **20**, 956–964.

Connors, B.W., Malenka, R.C. & Silva, L.R. (1988) Two inhibitory postsynaptic potentials, and GABAA and GABAB receptor-mediated responses in neocortex of rat and cat. *J. Physiol.*, **406**, 443–468.

D'Angelo, E., Nieus, T., Maffei, A., Armano, S., Rossi, P., Taglietti, V., Fontana, A. & Naldi, G. (2001) Theta frequency bursting and resonance in cerebellar granule cells: experimental evidence and modeling of a slow K^+-dependent mechanism. *J. Neurosci.*, **21**, 759–770.

D'Angelo, E., De Filippi, G., Rossi, P. & Taglietti, V. (1995) Synaptic excitation of individual rat cerebellar granule cells in situ: evidence for the role of NMDA receptors. *J. Physiol. (Lond.)*, **484**, 397–413.

D'Angelo, E., Rossi, P., Armano, S. & Taglietti, V. (1999) Evidence for NMDA and mGlu receptor-mediated long-term potentiation of mossy fibre-granule cell transmission in the rat cerebellum. *J. Neurophysiol.*, **81**, 277–287.

Debanne, D., Daoudal, G., Sourdet, V. & Russier, M. (2003) Brain plasticity and ion channels. *J. Physiol. Paris*, **97**, 403–414.

Dhamoon, A.S., Pandit, S.V., Sarmast, F., Parisian, K.R., Guha, P., Li, Y., Bagwe, S., Tafet, S.M. & Anumonwo, J.M.B. (2004) Unique Kir2.x properties determine regional and species differences in the cardiac inward rectifier K^+ current. *Circ. Res.*, **94**, 1332–1339.

Dieudonne, S. (1998) Submillisecond kinetics and low efficacy of parallel fibre-Golgi cell synaptic currents in the rat cerebellum. *J. Physiol.*, **510**, 845–866.

Dittman, J.S. & Regehr, W.G. (1997) Mechanism and kinetics of heterosynaptic depression at a cerebellar synapse. *J. Neurosci.*, **17**, 9048–9059.

Dugue, G.P., Dumoulin, A., Triller, A. & Dieudonne, S. (2005) Target-dependent use of coreleased inhibitory transmitters at central synapses. *J. Neurosci.*, **25**, 6490–6498.

Dutar, P. & Nicoll, R. (1988) A physiological role for $GABA_B$ receptors in the central nervous system. *Nature*, **332**, 156–158.

Edgley, S.A. & Lidierth, M. (1987) The discharges of cerebellar Golgi cells during locomotion in the cat. *J. Physiol. (Lond.)*, **392**, 315–332.

Hansel, C., Linden, D.J. & D'Angelo, E. (2001) Beyond parallel fiber LTD: the diversity of synaptic and non-synaptic plasticity in the cerebellum. *Nat. Rev. Neurosci.*, **4**, 467–475.

Hille, B. & Schwarz, W. (1978) Potassium channels as multi-ion single file pores. *J. Gen. Physiol.*, **72**, 409–442.

Hoang, Q.V., Zhao, P., Nakajima, S. & Nakajima, Y. (2004) Orexin (hypocretin) effects on constitutively active inward rectifier K+ channels in cultured nucleus basalis neurons. *J. Neurophysiol.*, **92**, 3183–3191.

Horio, Y., Morishige, K., Takahashi, N. & Kurachi, Y. (1996) Differential distribution of classical inwardly rectifying potassium channel mRNAs in the brain: comparison of CIRK2 with CIRK1 and CIRK3. *FEBS Lett.*, **379**, 239–243.

Horn, D. & Marty, A. (1988) Muscarinic activation of ionic currents measured by a new whole-cell recording method. *J. Gen. Physiol.*, **92**, 149–159.

Ige, A.O., Bolam, J.P., Billinton, A., White, J.H., Marshall, F.H. & Emson, P.C. (2000) Cellular and sub-cellular localisation of GABA(B1) and GABA(B2) receptor proteins in the rat cerebellum. *Brain Res. Mol. Brain Res.*, **83**, 72–80.

Inoue, M. & Imanaga, I. (1995) Phosphatase is responsible for run down, and probably G protein-mediated inhibition of inwardly rectifying K^+ currents in guinea pig chromaffin cells. *J. Gen. Physiol.*, **105**, 249–266.

Kamouchi, M., Van Den Bremt, K., Eggermont, J., Droogmans, G. & Nilius, B. (1997) Modulation of inwardly rectifying potassium channels in cultured bovine pulmonary artery endothelial cells. *J. Physiol. (Lond.)*, **504**, 545–556.

Karschin, C., Dissmann, E., Stuhmer, W. & Karschin, A. (1996) IRK(1–3) and GIRK(1–4) inwardly rectifying K^+ channel mRNAs are differentially expressed in the adult rat brain. *J. Neurosci.*, **16**, 3559–3570.

Kato, K. (1990) Novel $GABA_A$ receptor alpha subunit is expressed only in cerebellar granule cells. *J. Mol. Biol.*, **214**, 619–624.

Kofuji, P., Hofer, M., Millen, K.J., Millonig, J.H., Davidson, N., Lester, H.A. & Hatten, M.E. (1996) Functional analysis of the weaver mutant GIRK2 K^+ channel and rescue of weaver granule cells. *Neuron*, **16**, 941–952.

Lambolez, B., Audinat, E., Bochet, P., Crepel, F. & Rossier, J. (1992) AMPA receptor subunits expressed by single Purkinje cells. *Neuron*, **9**, 247–258.

Léna, C., de Kerchove d'Exaerde, A., Cordero-Erausquin, M., Le Novère, N., Arroyo-Jimenez, M.M. & Changeux, J.P. (1999) Diversity and distribution of nicotinic acetylcholine receptors in the locus ceruleus neurons. *Proc. Natl Acad. Sci. USA*, **96**, 12126–12131.

Leonoudakis, D., Conti, L.R., Radeke, C.M., McGuire, L.M. & Vandenberg, C.A. (2004) A multiprotein trafficking complex composed of SAP97, CASK, Veli, and Mint1 is associated with inward rectifier Kir2 potassium channels. *J. Biol. Chem.*, **279**, 19051–11963.

Leonoudakis, D., Mailliard, W., Wingerd, K., Clegg, D. & Vandenberg, C. (2001) Inward rectifier potassium channel Kir2.2 is associated with synapse-associated protein SAP97. *J. Cell Sci.*, **114**, 987–998.

Liang, F., Hatanaka, Y., Saito, H., Yamamori, T. & Hashikawa, T. (2000) Differential expression of gamma-aminobutyric acid type B receptor-1a and -1b mRNA variants in GABA and non-GABAergic neurons of the rat brain. *J. Comp. Neurol.*, **416**, 475–495.

Liao, Y.J., Jan, Y.N. & Jan, L.Y. (1996) Heteromultimerization of G-protein-gated inwardly rectifying K+ channel proteins GIRK1 and GIRK2 and their altered expression in weaver brain. *J. Neurosci.*, **16**, 7137–7150.

Marr, D. (1969) A theory of cerebellar cortex. *J. Physiol.*, **202**, 437–470.

Mathie, A., Clarke, C.E., Ranatunga, K.M. & Veale, E.L. (2003) What are the roles of the many different types of potassium channel expressed in cerebellar granule cells? *Cerebellum*, **2**, 11–25.

Mermelstein, P.G., Song, W.J., Tkatch, T., Yan, Z. & Surmeier, D.J. (1998) Inwardly rectifying potassium (IRK) currents are correlated with IRK subunit expression in rat nucleus accumbens medium spiny neurons. *J. Neurosci.*, **18**, 6650–6661.

Misgeld, U., Bijak, M. & Jarolimek, W. (1995) A physiological role for $GABA_B$ receptors and the effects of baclofen in the mammalian central nervous system. *Prog. Neurobiol.*, **46**, 423–462.

Mitchell, S.J. & Silver, R.A. (2000) Glutamate spillover suppresses inhibition by activating presynaptic mGluRs. *Nature*, **404**, 498–502.

Nicoll, R.A. (2004) My close encounter with $GABA_B$ receptors. *Biochem. Pharmacol.*, **68**, 1667–1674.

Pitzer, K.S. & Mayorga, G. (1973) Thermodynamics of electrolytes. II. Activity and osmotic coefficients for strong electrolytes with one or both ions univalent. *J. Phys. Chem.*, **77**, 2300–2308.

Porter, J.T., Cauli, B., Tsuzuki, K., Lambolez, B., Rossier, J. & Audinat, E. (1999) Selective excitation of subtypes of neocortical interneurons by nicotinic receptors. *J. Neurosci.*, **19**, 5228–5235.

Pruss, H., Derst, C., Lommel, R. & Veh, R.W. (2005) Differential distribution of individual subunits of strongly inwardly rectifying potassium channels (Kir2 family) in rat brain. *Brain Res. Mol. Brain Res.*, **139**, 63–79.

Rossi, P., De Filippi, G., Armano, S., Taglietti, V. & D'Angelo, E. (1998) The weaver mutation causes a loss of inward rectifier current regulation in premigratory granule cells of the mouse cerebellum. *J. Neurosci.*, **18**, 3537–3547.

Rossi, D.J., Hamann, M. & Attwell, D. (2003) Multiple modes of GABAergic inhibition of rat cerebellar granule cells. *J. Physiol. (Lond.)*, **548**, 97–110.

Schweighofer, N., Doya, K. & Lay, F. (2000) Unsupervised learning of granule cell sparse codes enhances cerebellar adaptive control. *Neuroscience*, **103**, 35–50.

Slesinger, P.A., Stoffel, M., Jan, Y.N. & Yan, L.Y. (1997) Defective g-aminobutyric acid type B receptor-activated inwardly rectifying K+ currents in cerebellar granule cells isolated from waver and Girk2 null mutant mice. *Proc. Natl. Acad. Sci. USA*, **94**, 12210–12217.

Stanfield, P.R., Nakajima, S. & Nakajima, Y. (2002) Constitutively active and G-protein coupled inward rectifier K^+ channels: Kir2.0 Kir3.0. *Rev. Physiol. Biochem. Pharmacol.*, **145**, 47–179.

Stonehouse, A.H., Pringle, J.H., Norman, R.I., Stanfield, P.R., Conley, E.C. & Brammar, W.J. (1999) Characterization of Kir2.0 proteins in the rat cerebellum and hippocampus by polyclonal antibodies. *Histochem. Cell Biol.*, **112**, 457–465.

Takano, K., Stanfield, P.R., Nakajiama, S. & Nakajiama, Y. (1995) Protein kinase C-mediated inhibition of an inward rectifier potassium channel by substance P in nucleus basalis neurons. *Neuron*, **14**, 999–1008.

Turrigiano, G.G. & Nelson, S.B. (2004) Homeostatic plasticity in the developing nervous system. *Nat. Rev. Neurosci.*, **5**, 97–107.

Velimirovic, B.M., Koyano, K., Nakajima, S. & Nakajima, Y. (1995) Opposing mechanisms of regulation of a G-protein-coupled inward rectifier K^+ channel in rat brain neurons. *Proc. Natl Acad. Sci. USA*, **92**, 1590–1594.

Vos, B.P., Maex, R., Volny-Luraghi, A. & De Schutter, E. (1999b) Parallel fibers synchronize spontaneous activity in cerebellar Golgi cells. *J. Neurosci.*, **19**, RC6 1–5.

Vos, B.P., Volny-Luraghi, A. & De Schutter, E. (1999a) Cerebellar Golgi cells in the rat: receptive fields and timing of responses to facial stimulation. *Eur. J. Neurosci.*, **11**, 2621–2634.

Wang, H.S. & McKinnon, D. (1996) Modulation of inwardly rectifying currents in rat sympathetic neurons by muscarinic receptors. *J. Physiol. (Lond.)*, **492**, 467–478.

Zhang, W. & Linden, D.J. (2003) The other side of the engram: experience-driven changes in neuronal intrinsic excitability. *Nat. Rev. Neurosci.*, **4**, 885–900.